



# University of HUDDERSFIELD

## University of Huddersfield Repository

Shen, Qiang, Ran, Guang, Hinks, Jonathan A., Donnelly, Stephen E., Wang, Lumin and Li, Ning

In situ observation of microstructure evolution in 4H-SiC under 3.5 keV He<sup>+</sup> irradiation

### Original Citation

Shen, Qiang, Ran, Guang, Hinks, Jonathan A., Donnelly, Stephen E., Wang, Lumin and Li, Ning (2016) In situ observation of microstructure evolution in 4H-SiC under 3.5 keV He<sup>+</sup> irradiation. *Journal of Nuclear Materials*, 471. pp. 149-153. ISSN 0022-3115

This version is available at <http://eprints.hud.ac.uk/27166/>

The University Repository is a digital collection of the research output of the University, available on Open Access. Copyright and Moral Rights for the items on this site are retained by the individual author and/or other copyright owners. Users may access full items free of charge; copies of full text items generally can be reproduced, displayed or performed and given to third parties in any format or medium for personal research or study, educational or not-for-profit purposes without prior permission or charge, provided:

- The authors, title and full bibliographic details is credited in any copy;
- A hyperlink and/or URL is included for the original metadata page; and
- The content is not changed in any way.

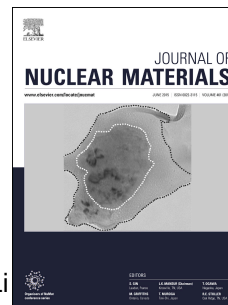
For more information, including our policy and submission procedure, please contact the Repository Team at: [E.mailbox@hud.ac.uk](mailto:E.mailbox@hud.ac.uk).

<http://eprints.hud.ac.uk/>

# Accepted Manuscript

*In situ* Observation of Microstructure Evolution in 4H-SiC under 3.5keV He<sup>+</sup> Irradiation

Qiang Shen, Guang Ran, Jonathan Hinks, Stephen E. Donnelly, Lumin Wang, Ning Li



PII: S0022-3115(16)30015-0

DOI: [10.1016/j.jnucmat.2016.01.017](https://doi.org/10.1016/j.jnucmat.2016.01.017)

Reference: NUMA 49558

To appear in: *Journal of Nuclear Materials*

Received Date: 3 July 2015

Revised Date: 16 January 2016

Accepted Date: 19 January 2016

Please cite this article as: Q. Shen, G. Ran, J. Hinks, S.E Donnelly, L. Wang, N. Li, *In situ* Observation of Microstructure Evolution in 4H-SiC under 3.5keV He<sup>+</sup> Irradiation, *Journal of Nuclear Materials* (2016), doi: 10.1016/j.jnucmat.2016.01.017.

This is a PDF file of an unedited manuscript that has been accepted for publication. As a service to our customers we are providing this early version of the manuscript. The manuscript will undergo copyediting, typesetting, and review of the resulting proof before it is published in its final form. Please note that during the production process errors may be discovered which could affect the content, and all legal disclaimers that apply to the journal pertain.

# ***In situ* Observation of Microstructure Evolution in 4H-SiC under 3.5keV He<sup>+</sup> Irradiation**

Qiang Shen<sup>a,b</sup>, Guang Ran<sup>a,\*</sup>, Jonathan Hinks<sup>b,\*</sup>, Stephen E Donnelly<sup>b</sup>, Lumin Wang<sup>a</sup>, Ning Li<sup>a</sup>

<sup>a</sup> College of Energy, Xiamen University, Xiamen, Fujian 361102, China

<sup>b</sup> School of Computing and Engineering, University of Huddersfield, Huddersfield HD1 3DH, United Kingdom

**Abstract:** 4H-SiC was irradiated with 3.5 keV He<sup>+</sup> ions using the MIAMI facility at University of Huddersfield. The evolution of microstructure and gas bubbles during the irradiation at 700°C, 800°C and 900°C was observed by *in situ* transmission electron microscopy. Under irradiation, isolated bubbles and bubble discs formed in the SiC matrix. Bubble discs lying on {0001} and {10-10} crystal planes were beginning to form at ion fluence above  $2.3 \times 10^{20}$  He<sup>+</sup>/m<sup>2</sup> at 700°C. The density of bubble discs increased with increasing irradiation fluence. However, growth rates were different at different of the implantation periods and temperature holding periods. The nucleation and growth of the bubble discs were attributed to be coalescence of the adjacent He vacancies and combination of loop punching and trap mutation, respectively.

**Key words:** SiC; *In situ* TEM; *In situ* irradiation; bubble disc; microstructure

---

\*Corresponding author: (Guang Ran) College of Energy, Xiamen University, Xiamen, Fujian 361005, China. Email: [gran@xmu.edu.cn](mailto:gran@xmu.edu.cn)(G.Ran);

\*(Jonathan Hinks) School of Computing and Engineering, University of Huddersfield, Huddersfield HD1 3DH, United Kingdom. Email: [j.a.hinks@hud.ac.uk](mailto:j.a.hinks@hud.ac.uk).

## 1 Introduction

Silicon carbide is considered as a promising candidate material used in nuclear energy due to its superior irradiation tolerance, high thermal conductivity, low thermal expansion, good thermal shock resistance and chemical inertness [1,2]. One of the most important applications is that SiC can be used as a structural layer in Tri-structural isotropic (TRISO) particles which have been used as nuclear fuel in high temperature gas-cooled reactors for several decades [3,4]. At present, TRISO particle fuels are also considered to be used in fluoride salt high temperature reactors and light water reactors [2,5]. After the catastrophic events at the Fukushima Dai-ichi nuclear reactors, ceramic accident tolerant fuel (ATF) systems utilizing SiC-based cladding have been under development as a potential replacement for zircaloy due to significantly low exothermic reaction with steam and their ability to retain a stable core geometry to very high temperature [6,7]. In the newly designed fully ceramic micro-encapsulated fuel (FCM) system, the TRISO particles are embedded in an additional fission product barrier of SiC matrix thus providing enhanced safety and superior irradiation resistance as compared to the traditional TRISO compact as well as UO<sub>2</sub> fuels [5,8]. SiC has been also proposed as a first wall material in fusion reactor [9,10]. Helium is inevitably introduced into the first wall material by energetic helium bombardment from the plasma and (*D,T*) reactions [11]. Helium atoms gather to form bubbles or bubble discs that may hasten the degradation of SiC-based materials.

Effects of helium irradiation on SiC have been widely investigated. Zhang *et al.* studied the helium fluence dependence of nanoscale cavity formation in 4H-SiC [12]. Helium bubbles were formed in 4H-SiC when helium was implanted at the room temperature, 227°C and 600°C. Planar bubble clusters were found when these He-implanted samples were annealed at temperature above 700°C. Hojou reported the helium bubbles were likely to be formed along the basal plane of

hexagonal SiC [13]. In Chen's work, He<sup>+</sup> implantation of hot-pressed SiC at ambient temperature resulted in the formation of helium platelets lying on {0001} planes [14,15]. Transformation from the platelet-shaped cavities into bubble discs was reported when irradiated samples were annealed at 1227°C. Bubble-loop complexes were formed when annealed temperature at 1427°C. Li *et al.* observed bubble discs associated with dislocation loops and stacking faults inside grains after post-irradiation annealing at 1000°C [16]. Texier *et al.* found the large cavities lying on {0001} and {10-10} are formed and experienced on transformation when the He irradiated 4H-SiC were annealed at 1700°C [17].

These large amount of *ex situ* experiment results of helium irradiation SiC are important for understanding of irradiation effects on SiC. However, these experiments cannot provide and display the temporally and spatially microstructure variation that are very important for the underline fundamental irradiation effect. Based on the characteristics of online facilities of accelerator and TEM, *in situ* observation was used to understand the evolution of microstructure. Pawley reported the evolution of bubbles in 4H-SiC by helium implantation at 700°C [18]. Hojou's *in situ* experiment demonstrated that the pre-implantation of hydrogen could enhance the formation and growth of helium bubbles in SiC [19]. Those studies provided rich microstructure evolution behaviors of SiC under ion irradiation. However, there are still some questions that need to be addressed, such as, the mechanism of the nucleation and growth of bubble discs. In the present work, the microstructure evolution behaviors of 4H-SiC by helium irradiation are investigated by *in situ* TEM in the temperature range of 700°C-900°C.

## 2 Experiment

4H-SiC single crystal from Cree Corporation, USA, was used in the present work. The

specimen surface is  $7.88^\circ$  off the (0001) plane. Both sides of each specimen were polished by diamond sand paper. After thinned to 10~15 $\mu\text{m}$ , specimen was glued on a molybdenum grid by G-1 epoxy glue. Then, specimen was thinned to about 100nm thickness by Ar ion milling using a Precision Ion Polishing System.

Helium ions were implanted into the 4H-SiC specimen at 700°C, 800°C and 900°C using the MIAMI facility at University of Huddersfield, UK [20]. The microstructure and gas bubble evolution was monitored *in situ* during helium ion irradiation using a 200keV electron beam. The ion flux and total ion fluence were  $2.5 \times 10^{17} \text{ He}^+ / (\text{m}^2 \cdot \text{s})$  and  $9.1 \times 10^{20} \text{ He}^+ / \text{m}^2$ , respectively. The incident angle of helium ion was  $30^\circ$  off the normal direction of specimen surface. The ion energy was designed as 3.5 keV by Monte Carlo calculation using the Stopping and Range of Ions in Matter (SRIM) software. The displacement energy of Si and C was assumed to be 35eV and 20eV, respectively. The depth of helium ion concentration peak and displacement damage peak are about 35nm and 15nm, respectively. The implantation helium concentration peak is about 26 at.% and peak displacement damage is 15.5 dpa after a fluence of  $9.1 \times 10^{20} \text{ He}^+ / \text{m}^2$ .

### 3 Results and discussion

Fig.1 shows under-focused TEM BF images of the 4H-SiC specimens irradiated by  $6.1 \times 10^{20} \text{ He}^+ / \text{m}^2$  fluence at (a) 700°C, (b) 800°C, and (c) 900°C. Specimens are viewed along the [0001] crystal direction. It can be seen that lots of isolated bubbles distribute in the SiC matrix at 700°C, 800°C and 900°C. However, a high density of bubble discs are observed at 800°C and 900°C with few at 700°C. Fringes with bright and dark contrast surrounding the bubble discs can be seen in the images. All TEM images in this work were taken at the same under-focused condition of 3.0 $\mu\text{m}$ .

The result is in good agreement with Zhang's ex situ experiment, where bubbles discs were

formed when the specimens were annealed above 700°C with a helium fluence of  $2.5 \times 10^{20}$  He<sup>+</sup>/m<sup>2</sup> [21]. It is speculated that a temperature threshold around 700°C may be the essential for the formation of bubble discs in 4H-SiC. Chen's post-implantation annealing experiments detected the formation of He platelet-shaped cavities at room temperature in polycrystalline SiC. Then helium platelets transformed to bubble discs after the sample had been annealed up to 1227°C [15]. However, in the present work, the transformation phenomenon was not observed. This may be due to the instantaneous transformation and the subtle contrast change between He platelets and bubble discs. The nucleation of platelet-shaped cavities at the early stage of the implantation is thought to be necessary for the formation of bubble discs. Both isolated bubbles and bubble discs are formed in the irradiated areas as shown in Fig.1. Thus, The isolated bubbles are in favor to be formed rather than platelet-shaped bubble discs if no platelets have been formed. Similar evolution behavior has been reported in He-implanted Mo although detailed mechanism remains in questions [22].

With increasing He<sup>+</sup> ion fluence, the bubble discs undergo significant growth at 800°C as shown in Fig. 2. Three bubble discs as indicated by white rectangles in Fig.2(a) were monitored during the ion irradiation. The average length of bubble discs increases from 10 nm to 30 nm when ion fluence increases from  $2.3 \times 10^{20}$  ions/m<sup>2</sup> to  $6.1 \times 10^{20}$  ions/m<sup>2</sup>. However, the bubble discs almost stop growing after ion fluence up to  $6.1 \times 10^{20}$  ions/m<sup>2</sup>. Even though SiC is further irradiated to  $9.1 \times 10^{20}$  ions/m<sup>2</sup> fluence, the average length of bubble discs still remain at 30nm. The relationship between the size of bubble discs and ion fluence is shown in Fig.3. The length and width of bubble discs increase significantly from  $2.3 \times 10^{20}$  ions/m<sup>2</sup> to  $4.6 \times 10^{20}$  ions/m<sup>2</sup>, and then slow down. The average width is about 3.3nm after irradiation with  $6.1 \times 10^{20}$  ions/m<sup>2</sup> fluence. During the experiment helium irradiation had been paused at a fluence of  $3.1 \times 10^{20}$  ions/m<sup>2</sup>,  $3.8 \times 10^{20}$  ions/m<sup>2</sup> and  $4.6 \times 10^{20}$  ions/m<sup>2</sup> for 6min, 16min and 15min, respectively. The bubble discs still keep growing even though

the helium irradiation is stopped. The length of #3 bubble disc increases from 7.5nm to 17.5nm at only 6min pause after irradiation with  $3.1 \times 10^{20}$  ions/m<sup>2</sup> as shown in Fig.4(a). Correspondingly, the width of #3 bubble disc increases from 1.8nm to 2.7nm as shown in Fig.4(b). The similar growth of other two bubble discs during the implantation and temperature holding periods are observed as shown in Fig.3 and Fig.4.

The pressures inside the isolated bubbles and the bubble discs should be balanced during helium irradiation in consideration of the co-existence of the isolated bubbles and the bubble discs in the range of 700-900°C. Based on the profile of SRIM calculation, almost all implanted helium remain in the specimen. According to Pawley's work[18], less than 10% of implanted helium atoms form bubbles and bubble discs after irradiation with  $4.6 \times 10^{20}$  ions/m<sup>2</sup>. Thus, other parts of helium atoms exist as interstitial atoms and invisible helium clusters in SiC matrix. The interstitial helium atoms have high mobility and the vacancies have low mobility in SiC in the range of 700-900°C [14,15]. Pramono indicated that helium atoms were most likely to diffuse by dissociative/interstitial mechanism in this temperature range [23]. The growth rates of the bubble discs are calculated as shown in Fig.5. It can be seen that #2 and #3 bubble discs show biggest growth rates under the annealing procedure after irradiation with  $3.1 \times 10^{20}$  ions/m<sup>2</sup>. The high ion flux causes serious damage at the beginning of stage. The heat effect provides the recombination of Frankel pairs of Si/C interstitials and Si/C vacancies and the diffusion of helium interstitials. This leads to the high growth rate of bubble discs during the temperature holding time between fluences of  $3.1 \times 10^{20}$  ions/m<sup>2</sup> and  $3.8 \times 10^{20}$  ions/m<sup>2</sup>. When the sample was irradiated with a fluence more than  $3.8 \times 10^{20}$  ions/m<sup>2</sup>, the growth rates during the implantation periods become relatively bigger than those during the temperature holding periods. The implantation introduced more helium atoms into the irradiated area so that the bubble discs continued to grow.



The bubble discs are believed to be evolved from helium trapped vacancy clusters, which can be written as  $\text{He}_x\text{V}_y$ , for example,  $\text{He}_2\text{V}$ ,  $\text{He}_3\text{V}$ ,  $\text{He}_4\text{V}_2$  (V is short for vacancy) [24,25]. Although the system is in favor of low energy facets rather than spherical bubbles with higher surface energy for the helium-implanted materials [26], both spherical bubbles and two dimensional bubble discs were formed in the present work. Therefore, it can be considered that the location of helium trapped vacancy clusters in the lattice and the distance between these vacancy clusters may affect the different nucleation of isolate bubble and bubble discs in SiC. Those vacancy clusters, which are generated near specific low energy planes, are able to coalesce together. The lattice atoms between them can be kicked out by trap mutation to turn into interstitials. The interstitial C and Si atoms have a migration energy of 0.74 eV and 1.53 eV [27], respectively, which is much lower than the migration energy of C vacancies (3.2-3.6 eV) and S vacancies (3.5-5.2eV) [28]. These interstitial C and Si atoms can be trapped between specific low energy planes to form interstitial dislocation loops, for example, (0001) and (10-10) planes. These coalesced vacancy clusters surrounding by interstitial dislocation loops act as nuclei of helium platelets. Once the nuclei are formed, they will grow by loop punching. Meanwhile, trap mutation process takes place at the edge of the platelets. The growth of bubble discs could be explained by these two processes. Furthermore, both of two processes are driven through the relaxation of inner pressure of the platelets. The inner helium pressure dropped discontinuously during these processes [29]. This may lead to the collapse of helium platelets. The transformation from platelets to bubble discs occurs after the collapse and some of the interstitial atoms return back into the lattice sites. It is believed that a cluster of small spherical bubbles have lower energy than a single platelet [22].

Specimen implanted with a fluence of  $9.1 \times 10^{20}$  ions/ $\text{m}^2$  at  $900^\circ\text{C}$  was cooled down to the room temperature. The bubble discs stay stable so that it is easier to analyze the distribution of the

orientation of bubble discs. The bubble discs are found to preferentially locate on some specific planes. A Gaussian multi-peak distribution gives a best fit for the distribution of the orientation of edge-on bubble discs as shown in Fig. 6. The angles are measured with respect to the positive horizontal direction of the TEM images. The peaks appear at angles of  $35^\circ$ ,  $100^\circ$  and  $157^\circ$ . The angle separation between these peaks is approximately  $60 \pm 5^\circ$ . The habit planes are  $\{-1100\}$ ,  $\{10-10\}$  and  $\{01-10\}$  planes, which are equivalent prismatic planes.

The helium platelets/bubble discs have also been found in some other materials irradiated by helium, such as in Mo [19,30], Ni [31], Ti [32] and  $B_4C$  [33]. Platelets/bubble discs in Mo with BCC structure lied on  $\{110\}$  close-packed planes [19]. For Ni with FCC structure, the platelets lied on  $\{111\}$  close-packed planes [31]. In Ti with HCP structure, platelets lied on  $\{0001\}$  basal planes [32]. However, platelets/bubble discs in SiC preferentially lied on  $\{0001\}$  planes [13,21] and  $\{10-10\}$  planes [17]. Consequently, the helium platelets are expected to nucleate preferentially on the close-packed planes that have largest distance between the two lattice layers and have least activation energy for the mutation trap process.

## 4 Conclusions

*In situ* TEM has been used to study irradiation effects and He bubble formation in 4H-SiC under 3.5keV  $He^+$  ion irradiation. The experimental results show that large amounts of bubble discs combined with isolated bubbles were formed in the 4H-SiC irradiated at 800 and 900°C with significantly fewer at 700°C. Bubble discs lying on  $\{0001\}$  and  $\{10-10\}$  crystal planes were beginning to form at ion fluence above  $2.3 \times 10^{20} He^+/m^2$  at 700°C. The density of bubble discs increased with increasing irradiation fluence. However, growth rates were different at different of the implantation periods and temperature holding periods. The nucleation and growth of the bubble discs were attributed to be coalescence of the adjacent He vacancies and combination of loop

punching and trap mutation, respectively.

## Acknowledgements

The work was supported by National Natural Science Foundation of China, through Grant No. 11305136.

## References

- [1] Y. Katoh, L.L. Snead, I. Szlufarska, W.J. Weber, *Curr. Opin. Solid State Mater. Sci.* 16 (2012) 143.
- [2] L.L. Snead, T. Nozawa, Y. Katoh, T.-S. Byun, S. Kondo, D.A. Petti, *Handbook of SiC Properties for Fuel Performance Modeling*, 2007.
- [3] J.J. van der Merwe, *J. Nucl. Mater.* 395 (2009) 99.
- [4] P. Hosemann, J.N. Martos, D. Frazer, G. Vasudevamurthy, T.S. Byun, J.D. Hunn, B.C. Jolly, K. Terrani, M. Okuniewski, *J. Nucl. Mater.* 442 (2013) 133.
- [5] K.A. Terrani, L.L. Snead, J.C. Gehin, *J. Nucl. Mater.* 427 (2012) 209.
- [6] K. Barrett, S. Bragg-Sitton, D. Galicki, *Advanced LWR Nuclear Fuel Cladding System Development Trade-off Study*, 2012.
- [7] P. Alto, *PWR Cores with Silicon Carbide Cladding*, 2001.
- [8] F. Venneri, Y.S. Kim, K.A. Terrani, A. Ougouag, J.E. Tulenko, C.W. Forsberg, P.F. Peterson, E.J. Lahoda, *Transactions of the American Nuclear Society*, 104(2011)668 .
- [9] A.R. Raffray, L. El-Guebaly, S. Gordeev, S. Malang, et al., *Eng. Des.*, 58–59 (2001)549.
- [10] L. Giancarli, H. Golfier, S. Nishio, R. Raffray, C. Wong, R. Yamada, *Eng. Des.*, 61–62 (2002)307.
- [11] J. Chen, P. Jung, H. Ullmaier, *J. Nucl. Mater.* 336 (2005) 194.

- [12] C.H. Zhang, S.E. Donnelly, V.M. Vishnyakov, J.H. Evans, *J. Appl. Phys.* 94 (2003) 6017.
- [13] K. Hojou, K. Izui, *J. Nucl. Mater.* 160 (1988) 147.
- [14] J. Chen, P. Jung, H. Trinkaus, *Phys. Rev. B* 61 (2000) 923.
- [15] J. Chen, P. Jung, H. Trinkaus, *Phys. Rev. Lett.* 82 (1999) 2709.
- [16] B.S. Li, Y.Y. Du, Z.G. Wang, K.F. Wei, H.P. Zhang, et al., *Vacuum* 113 (2015) 75.
- [17] M. Texier, B. Pichaud, M.F. Beaufort, J.F. Barbot, *J. Phys. D. Appl. Phys.* 46 (2013) 485105.
- [18] C. Pawley, *The Use of in-Situ Ion-Irradiation / TEM Techniques to Study Radiation Damage in SiC*, University of Salford, 2013.
- [19] K. Hojou, S. Furuno, K.N. Kushita, H. Otsu, K. Izui, *J. Nucl. Mater.* 191-194 (1992) 583.
- [20] J. A. Hinks, J. A. van den Berg, S.E. Donnelly, *J. Vac. Sci. Technol. A* 29 (2011) 021003.
- [21] C.H. Zhang, S.E. Donnelly, V.M. Vishnyakov, J.H. Evans, T. Shibayama, Y.M. Sun, *Nucl. Instr. Meth. B* 218 (2004) 53.
- [22] M.W. Finnis, A. Van Veen, L.M. Caspers, *Radiat. Eff.* 78 (1983) 121.
- [23] Y. Pramono, K. Sasaki, T. Yano, *J. Nucl. Sci. Technol.* 41 (2004) 751.
- [24] J.H. Evans, A. Van Veen, L.M. Caspers, *Radiat. Eff.* 78 (1983) 105.
- [25] A. Van Veen, J.H. Evans, W.T.M. Buters, L.M. Caspers, *Radiat. Eff.* 78 (2006) 53.
- [26] Q.M. Wei, N. li, K. Sun, L.M. Wang, *Scripta Mater.* 63 (2010) 430.
- [27] F. Gao, W. J. Weber, M. Posselt, V. Belko, *Phys. Rev. B* 69 (2004) 245205.
- [28] M. Bockstedte, A. Mattausch, O. Pankratov, *Phys. Rev. B* 69 (2004) 1.
- [29] H. Trinkaus, *Radiat. Eff.* 78 (1983) 189.
- [30] J.H. Evans, A. Van Veen, L.M. Caspers, *Nature* 291 (1981) 310.
- [31] M. D'Olieslaeger, L. De Schepper, G. Knuyt, L.M. Stals, *J. Nucl. Mater.* 138 (1986) 27.
- [32] Trinkaus, *Philos. Mag. A* 65 (1992) 1235.

[33] A. Jostsons, C.K.H. DuBose, G. Copeland, J.O. Stiegler, J. Nucl. Mater. 49 (1973) 136.

## Figure Captions

Fig.1 Under-focused TEM BF images of the 4H-SiC irradiated by  $6.1 \times 10^{20}$  He<sup>+</sup>/m<sup>2</sup> fluence at (a) 700°C, (b) 800°C, and (c) 900°C, respectively. Direction of observation is the [0001] crystal direction.

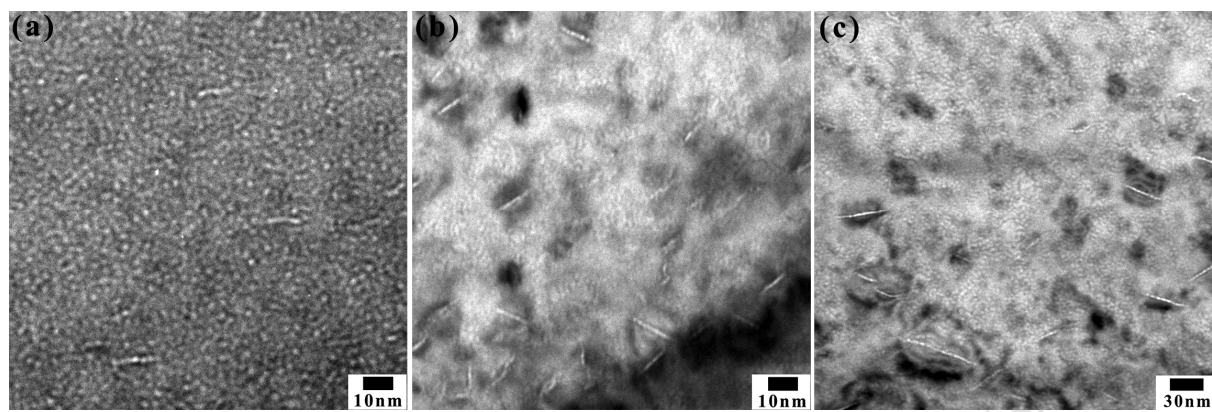
Fig.2 The growth of edge-on bubble discs at 800°C with different ion fluence: (a)  $2.3 \times 10^{20}$  ions/m<sup>2</sup>, (b)  $6.1 \times 10^{20}$  ions/m<sup>2</sup>. Scale bar in (a) applies to both (a) and (b). Direction of observation is the [0001] crystal direction.

Fig.3 The relationship between the size of bubble discs and ion fluence at 800°C, (a) Length vs. fluence; (b) Width vs. fluence. The pause time after ion implantation with  $3.1 \times 10^{20}$  ions/m<sup>2</sup>,  $3.8 \times 10^{20}$  ions/m<sup>2</sup> and  $4.6 \times 10^{20}$  ions/m<sup>2</sup> is 6min, 16min and 15min, respectively.

Fig.4 The relationship between the size of bubble discs and pause time after ion implantation with  $3.1 \times 10^{20}$  ions/m<sup>2</sup> at 800°C, (a) Length vs. pause time; (b) Width vs. pause time

Fig.5 The growth rate of bubble discs during the implanting time and holding time.

Fig.6 Distribution of the angles of the bubble discs at 900°C after irradiation with  $6.1 \times 10^{20}$  ions/m<sup>2</sup> and corresponding Gaussian fitting curve.



ACCEPTED MANUSCRIPT

